Biochimica et Biophysica Acta, 1150 (1993) 17–24

BBAMEM 76011

FTIR analysis of nicotinic acetylcholine receptor secondary structure in reconstituted membranes

Daniel H. Butler and Mark G. McNamee

Department of Biochemistry and Biophysics, University of California at Davis, Davis, CA (USA)

(Received 6 June 1992)
(Revised manuscript received 13 January 1993)

Key words: Nicotinic acetylcholine receptor; FTIR; Secondary structure; Lipid–protein interaction; Desensitization; (*T. californica*)

Using Fourier-transform infrared resonance spectroscopy, we examined the structure of the purified *Torpedo californica* nicotinic acetylcholine receptor in reconstituted dioleoylphosphatidylcholine membranes in H_2O and D_2O. Using the amide-I band, we calculated the secondary structure of nAChR in H_2O to be approx. 19% α-helix, 42% β-structure, 24% turns and 15% unordered. The secondary structure content in D_2O was estimated to be 14% α-helix, 37% β-structure, 29% turns and 20% unordered. In the presence of phosphatidic acid the β-structure content in D_2O increased significantly from 37% to 42%. This suggests that an ionic interaction between negatively-charged lipid head groups and positively-charged peptide side chains may stabilize a β-structure conformation that is necessary for receptor function. The inclusion of cholesterol in the reconstituted membranes significantly increased the α-helix content from 14% to 17%. These results support the hypothesis that cholesterol may induce a transmembrane region to undergo a unordered-to-helix transition which is necessary to maintain the integrity of the ion channel. Additionally, we found that nAChR did not undergo major secondary structure changes when subjected to conditions that induce desensitization. This is consistent with the view that the mechanism of desensitization consists of small quaternary rearrangements of the subunits rather than large changes in receptor secondary structure.

Introduction

The nicotinic acetylcholine receptor (nAChR) of the marine electric fish, *Torpedo californica*, is the best-characterized member of a superfamily of ligand-gated ion channels. This class of membrane proteins includes mammalian muscle and neuronal nAChRs, as well as the $GABA_A$, glutamate and glycine receptors [1]. The results obtained by investigating the structure and function of the *Torpedo* nAChR should assist in characterizing other receptors in its class.

Torpedo nAChR is a pentameric integral membrane protein located on the postsynaptic membrane of the electroplax cells. The receptor is composed of two alpha subunits and a single copy of the homologous beta, gamma, and delta subunits [2]. Upon binding a molecule of acetylcholine on each alpha subunit, the receptor changes conformation to open an ion channel across the lipid bilayer [3]. The influx of cations causes a depolarization event that subsequently triggers an electric discharge from the fish.

Each subunit is believed to contain four helical transmembrane crossings which are denoted as the M1, M2, M3 and M4 [4]. The ion channel lies in the center of the pentamer with the M2 helix lining the pore [5,6]. Although the M4 helix lies furthest from the channel, it is possibly important for channel gating [7, 8]. The functional role of the M1 and M3 helices are still unknown.

The functional aspects of nAChR have been investigated extensively. nAChR has been used as a model system to determine how lipid-protein interactions can modulate receptor activity. Previous studies have established that nAChR requires the presence of negatively charged phospholipids (such as phosphatidic acid) and cholesterol in order to retain optimal ion-flux function [9–11]. Spin-labeling studies have demonstrated that phosphatidic acid has a relatively high affinity for the receptor [12]. nAChR can also alter the pK_a values of the phosphatidic acid head groups at the lipid/protein interface, suggesting that an ionic interaction may be

Correspondence to: M.G. McNamee, Department of Biochemistry and Biophysics, University of California at Davis, Davis, CA 95616, USA.

Abbreviations: FTIR, Fourier-transform infrared; nAChR, nicotinic acetylcholine receptor; PC, dioleolylphosphatidylcholine; PA, dioleoylphosphatidic acid; CH, cholesterol; D_2O, deuterium oxide.

occurring between charged protein side chains and lipid moieties at the surface of the bilayer [41].

nAChR has also been the focus of desensitization studies. In the prolonged presence of activating ligands, nAChR undergoes a loss of response to further addition of ligand [13]. A variety of ligands are believed to bind to the receptor and shift it into desensitized state [13]. Structural studies have been performed to determine how the conformation of the desensitized receptor differs from the resting conformation [14,15].

In order to understand the molecular basis of desensitization and lipid–protein interactions, accurate structural models must be developed. However, nAChR, like most integral membrane proteins, is resistant to crystallization and high-resolution X-ray crystallographic analysis has not been possible. Indirect methods of structure analysis such as circular dichroism [16], electron microscopy [17] and low resolution X-ray diffraction [18] have been employed, but have provided only a primitive view of nAChR structure. Biophysical and molecular genetic approaches are being utilized to further refine this structural model.

An important element in creating an accurate structural model is to estimate the type and amount of secondary structure in the protein. A technique that has been increasing employed for this purpose is Fourier-transform infrared spectroscopy (FTIR). Within the last decade, FTIR has provided secondary structure data for many soluble proteins and these data are generally in good agreement with the available crystallographic structures [19]. The FTIR technique is now being extended to determine the secondary structure of integral membrane proteins that cannot be characterized by crystallographic analysis. Due to the lack of a membrane protein structure database, the accuracy of FTIR has not been assesed for this class of proteins. However, it is highly likely that the properties of the main elements of secondary structure will be similar among all protein classes.

In this paper, we perform FTIR studies to estimate the secondary structure of nAChR using the amide-I band and examine the lipid-dependent changes in structure that can be correlated with functional effects. The results of the present work are discussed in the context of the current models of receptor structure.

Materials and Methods

Acetylcholine receptor purification. nAChR was purified from *Torpedo californica* electroplax tissue by affinity chromatography [11]. nAChR purity was established by SDS-gel electrophoresis. Synthetic dioleoylphosphatidylcholine (PC) and dioleoylphosphatidic acid (PA) were obtained from Avanti Polar Lipids (Birmingham, AL, USA). The receptor was reconstituted into pure PC or a PC/PA mixture at a 50:50 molar ratio. Preparation of re-reconstituted PC/PA/cholesterol membranes at a 60:20:20 molar ratio was performed as described in Ref. 20. Protein and phosphate assays were utilized to determine the lipid-to-protein ratios which ranged from 200:1 to 500:1 [21,22]. All experiments were performed with DB-1 (100 mM NaCl, 10 mM Mops, 0.1 mM EDTA, 0.02% NaN_3 (pH 7.4)) as the buffer using either H_2O or D_2O as the solvent. Receptor samples were stored under liquid nitrogen until ready for use.

Preparation of nAChR samples for FTIR spectroscopy. For nAChR samples in H_2O, 1 mg of the purified receptor was centrifuged at $257\,000 \times g$ for 1 h to pellet the protein sample. For D_2O samples, purified nAChR was lyophilized overnight and D_2O was added to bring the samples to 1 mg/ml. They were incubated for 1 or 8 days at 4°C to facilitate deuterium exchange. The samples were then centrifuged as outlined above. 2 μl of DB-1 buffer were mixed with the pellet and a portion of the sample was placed between two calcium fluoride windows separated by a 15-mm Teflon spacer from Spectra-Tech (Stamford, CT, USA). For the ligand binding studies, 2 μl of 100 mM carbamylcholine chloride in DB-1 buffer was mixed with the pellet. The Perkin-Elmer 1750 FTIR spectrometer was purged with nitrogen gas to remove atmospheric water vapor and 100 scans were recorded at 4 cm^{-1} resolution.

Analysis of FTIR spectra. The DB-1 buffer spectra were subtracted from the original spectra so that a flat baseline was obtained between 1950–1750 cm^{-1} [23,24]. The lipid components were not subtracted because it was determined that they do not absorb appreciably in the amide-I or amide-II regions (data not shown). The subtracted spectra were smoothed with a Savitsky-Golay function [25]. Smoothing had negligible effects on the deconvolution of the amide-I band (data not shown). Utilizing Lab Calc data analysis software from Galactic Industries (Salem, NH, USA), these subtracted and smoothed spectra (corrected spectra) were deconvolved using parameters of $\gamma = 4.2$ and $X = 0.23$ or restored by the program SSRes using a Gaussian of width 12 cm^{-1} and uncertainty estimate of 2. The corrected, deconvolved, and restored spectra were subjected to a curve fitting procedure with Lab Calc using the procedures described in Byler and Susi [19]. Gaussian bands with a width of 12 cm^{-1} and peak centers from the second derivative spectra were used as initial input parameters for the curve-fit of each spectrum. The iterative procedure yielded the areas of the bands in the amide-I envelope. Although each component of the amide-I possesses different extinction coefficients, Byler and Susi have confirmed the validity of this analysis by comparing the secondary structure data against X-ray crystallographic structures. Each peak was assigned a particular secondary structure depend-

ing on its peak center [19,23]. The areas of the peaks with the same secondary structure were added together and divided by the sum of the areas of all assigned peaks in the amide-I to receive the relative secondary structure values. Each experiment was repeated two or three times. The secondary structure values were subjected to an unpaired Mann-Whitney *U*-test from the program Instat (GraphPAD Software, San Diego, CA, USA) to determine if the differences were statistically significant.

Secondary structure predictions. The *Torpedo californica* nAChR sequences were obtained from Noda et al. [26]. Estimates of nAChR structure were performed with the GCG Sequence Analysis Software Package-Version 7.0 [27]. This program used the modified Chou-Fasman prediction algorithm [28] developed by Nishikawa [29]. The Garnier-Osguthorpe-Robson (GOR) prediction method was also utilized for secondary structure estimates [30]. For this method, the minimum length of helix was set at six residues while the minimum β-structure length was set at four residues.

Results

Deuterium-exchange properties of nAChR

FTIR spectra of nAChR in dioleoylphosphatidylcholine membranes (nAChR-PC) were obtained in H_2O and D_2O (Fig. 1). Peptide chains absorb in three distinct areas in the interval between 4000 cm^{-1} and 1000 cm^{-1}. These bands are denoted as the amide-I, amide-II and amide-III envelopes. Absorptions in the amide-I region, located between 1700–1600 cm^{-1}, are due to the C-O stretch of the peptide backbone which is coupled to the adjacent N-H and C-N stretching

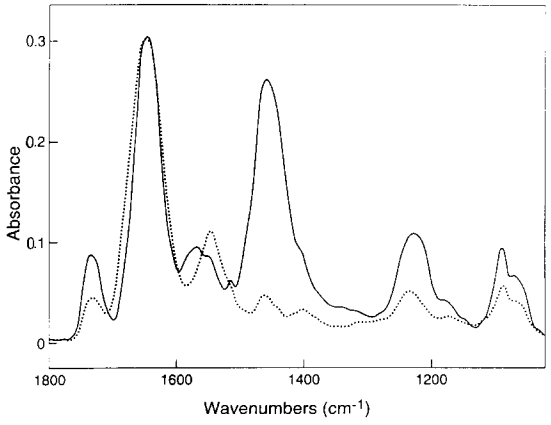

Fig. 1. Corrected FTIR spectra of nAChR-PC in H_2O (···) and nAChR-PC in D_2O (———). The amide-I band, between 1700–1600 cm^{-1}, narrowed and shifted to the right upon deuteration. The amide-II band centered at 1550 cm^{-1} in H_2O decreased in intensity in D_2O. A portion of the amide-III band which lies between 1100–900 cm^{-1} is shown. The P-O stretch of the phospholipid head group absorbs appreciably in this region.

TABLE I

Amide-I second derivative peak centers and assigned structure for nAChR-PC in H_2O and D_2O

Each nAChR-PC pellet containing approx. 1 mg of protein was mixed with 2 μl of buffer, placed between CaF_2 windows and scanned with an FTIR spectrometer. After spectral subtraction of buffer, the spectrum was subjected to second derivative analysis to obtain peak positions. The peaks were assigned a secondary structure element according to its center [19,23].

Peak center (cm^{-1})		Structure
H_2O	D_2O	
1693	1692	Turns
1683	1680	Turns
1674	1670	β-Structure
1665	1659	Turns
1656	1651	α-Helix
1647	1642	Unordered
1638	1632	β-Structure
1628	1624	β-Structure
1691	1619	Side chains
1609	1609	Side chains

modes [31]. Upon exchange of the amide protons with the heavier deuterium atom, the amide-I band narrows and the center shifts slightly from 1649 cm^{-1} to 1644 cm^{-1}. The amide-II band, centered at 1550 cm^{-1} in H_2O, decreases in intensity upon deuterium exchange. The intensity of this band is often used to estimate the degree of solvent exchange [32]. The amide-III band, located between 1100–900 cm^{-1}, arises from peptide skeletal vibrations which can also be assigned to secondary structure elements [31].

The subtracted and smoothed spectra recorded for nAChR-PC in both H_2O and D_2O were subjected to second derivative analysis allowing the individual peaks making up the amide-I envelope to be resolved. In Table I the peak centers are displayed for the H_2O and D_2O samples. All but two peaks shifted to a lower wavenumber upon treatment with D_2O solvent. The 1619 cm^{-1} and 1609 cm^{-1} bands were not displaced and are probably absorbances of side chains that are not coupled to exchangeable protons. These results are in good agreement with the 1–6 cm^{-1} downward shifts observed in other studies [33]. The deuterium exchange seems to be completed within 24 h as further changes in the spectrum are not evident even after 8 days (data not shown).

nAChR secondary structure

Secondary structure classifications have been assigned to amide-I bands according to their wavenumber as described in Materials and Methods (Table I). The second derivative spectra of nAChR-PC demonstrate that significant fractions of many secondary structure components are present in the receptor (Fig. 5). In order to quantify the relative amount of sec-

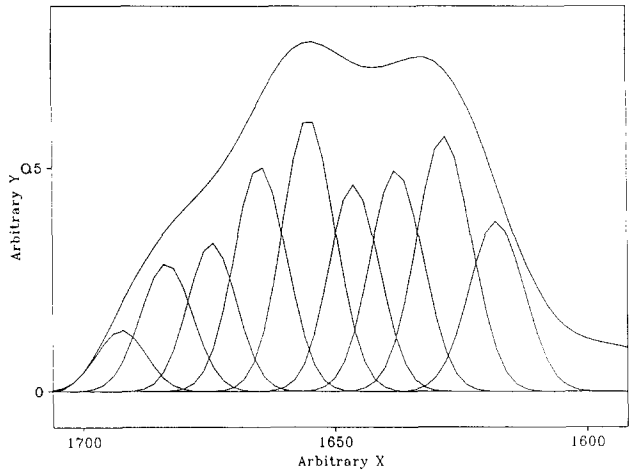

Fig. 2. Spectrum of nAChR-PC in H_2O upon deconvolution and curve-fitting. Each Gaussian band that composes the amide-I envelope is assigned to a secondary structure type. From left to right, turns 1693 cm^{-1} and 1683 cm^{-1}; β-structure 1674 cm^{-1}; turns 1665 cm^{-1}; α-helix 1656 cm^{-1}; unordered 1647 cm^{-1}; β-structure 1638 cm^{-1} and 1628 cm^{-1}.

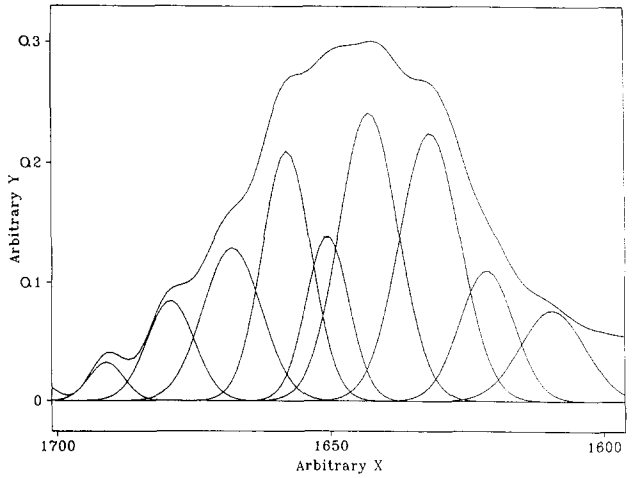

Fig. 3. Spectrum of nAChR-PC in D_2O upon deconvolution and curve-fitting. From left to right, the bands that composes the amide-I envelope; turns 1692 cm^{-1} and 1680 cm^{-1}; β-structure 1670 cm^{-1}; turns 1659 cm^{-1}; α-helix 1651 cm^{-1}; unordered 1642 cm^{-1}; β-structure 1631 cm^{-1}.

ondary structure, we curve-fit the corrected, deconvolved, and restored spectra (Figs. 2 and 3). Upon curve-fitting, we found excellent agreement between the secondary structure values obtained by the deconvolution and restoration procedures (Table II). These two independent procedures were used to verify proper transformation of the corrected spectra. As an additional precaution, the corrected spectra were also subjected to a curve-fit analysis. The values determined from the corrected spectra were also similar to the deconvolved and restored spectra (Table II).

Since the values obtained from the deconvolved and restored spectra were comparable, we averaged the two results to get a final secondary structure estimate. nAChR-PC in H_2O was determined to have a secondary structure content of $18.7 \pm 0.8\%$ α-helix, $42.0 \pm 0.6\%$ β-structure, $24.4 \pm 2.0\%$ turns and $14.5 \pm 1.5\%$ unordered (Table III). In D_2O, it was estimated that the receptor had $14.2 \pm 1.6\%$ α-helix, $37.0 \pm 1.5\%$ β-structure, $28.5 \pm 1.9\%$ turns and $20.2 \pm 2.7\%$ unordered. The differences in secondary structure values between the two samples are probably due to incomplete deuterium exchange of the transmembrane regions.

nAChR structure is affected by lipid environment

AChR was reconstituted into membranes containing PC, PCPA, and PCPACH and then subjected to FTIR analysis in D_2O solvent (Fig. 4). These experiments were performed to determine if specific lipids could alter the secondary structure of the receptor.

Our present studies show a significant change in the

TABLE II

Relative percentage of secondary structural elements for nAChR-PC in H_2O and in D_2O obtained by curve-fitting the corrected, deconvolved and restored spectra

The corrected spectra were deconvolved with using parameters of $\gamma = 4.2$ and $X = 0.23$ or restored by the program SSRes using a Gaussian of width 12 cm^{-1} and uncertainty estimate of 2. Gaussian bands with a width of 12 cm^{-1} and peak centers from the second derivative spectra were used as initial input parameters for the curve-fitting. The average value was computed from deconvolved and restored samples and represented as the mean $\pm$S.D.

Structure	Corrected	Deconvolved	Restored	Average
H_2O				
α-Helix	$16.0 \pm 0.8\%$	$18.8 \pm 0.7\%$	$18.6 \pm 1.1\%$	$18.7 \pm 0.8\%$
β-Structure	$41.9 \pm 0.2\%$	$42.1 \pm 0.8\%$	$41.9 \pm 0.5\%$	$42.0 \pm 0.6\%$
Turns	$27.2 \pm 1.8\%$	$25.9 \pm 1.6\%$	$23.0 \pm 0.8\%$	$24.4 \pm 2.0\%$
Unordered	$15.1 \pm 0.8\%$	$13.2 \pm 0.0\%$	$15.8 \pm 0.5\%$	$14.5 \pm 1.5\%$
D_2O				
α-Helix	$13.5 \pm 0.6\%$	$14.7 \pm 1.6\%$	$13.7 \pm 1.7\%$	$14.2 \pm 1.6\%$
β-Structure	$36.3 \pm 1.1\%$	$36.7 \pm 1.9\%$	$37.2 \pm 1.4\%$	$37.0 \pm 1.5\%$
Turns	$28.7 \pm 3.5\%$	$28.3 \pm 2.1\%$	$28.7 \pm 2.0\%$	$28.5 \pm 1.9\%$
Unordered	$21.5 \pm 2.0\%$	$20.1 \pm 3.1\%$	$20.2 \pm 2.9\%$	$20.2 \pm 2.7\%$

TABLE III

Secondary structure values for nAChR as determined by other techniques

FTIR amide-I values from nAChR-PC in H_2O were obtained as described in Materials and Methods. Chou-Fasman and GOR secondary structure prediction methods were performed with GCG software [27] with sequences provided by Ref. 26.

Method	α-Helix	β-Structure	Turns	Unordered
FTIR amide I [a]	19%	42%	24%	15%
Chou-Fasman [a]	29%	41%	15%	15%
GOR Prediction [a]	29%	28%	19%	23%
FTIR amide III [b]	17%	20%	n.d.	n.d.
Raman [c]	25%	34%	15%	24%
Circular dichroism [d]	23%	43%	6%	28%

[a] Data presented in this paper.
[b] nAChR reconstituted in pure PC membranes [34].
[c] nAChR reconstituted in pure PC membranes [40].
[d] nAChR reconstituted in asolectin [16].

β-structure content of nAChR in the presence of phosphatidic acid. The corrected spectra of nAChR-PCPA showed a slight downfield broadening of the amide-I band as compared to the amide-I envelope of nAChR-PC (Fig. 5). The second derivative spectrum of nAChR-PC in D_2O had a large peak assigned to β-structure centered at 1631 cm^{-1}. In the presence of phosphatidic acid (nAChR-PCPA), the β-structure band split into two peaks centered at 1633 cm^{-1} and 1626 cm^{-1} (Fig. 6). When the restored spectrum was curve-fit taking into account these new peak parameters, it was revealed that the β-structure content increased in D_2O from 37.0% in nAChR-PC to 42.3%, while the α-helix content showed only minor changes (Table IV). The band splitting and similar increase in β-structure were also evident in nAChR samples reconstituted in membranes consisting of PC/PA/cholesterol (nAChR-PCPACH). The Mann-Whitney *U*-test determined that the β-structure content of the samples

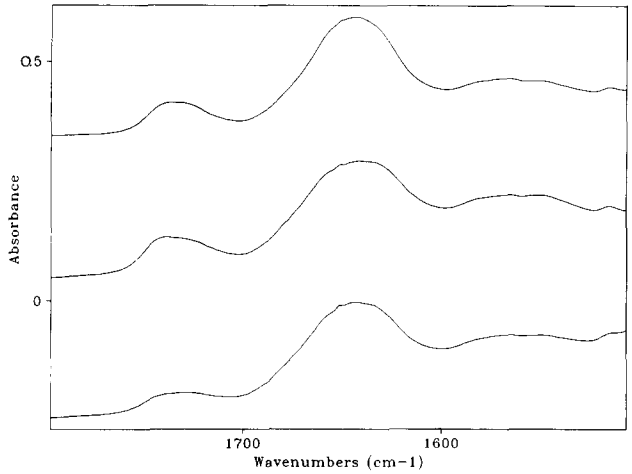

Fig. 4. Original unsmoothed and unsubtracted FTIR spectra of nAChR in D_2O solvent. From top to bottom: nAChR-PC, nAChR-PCPA and nAChR-PCPACH.

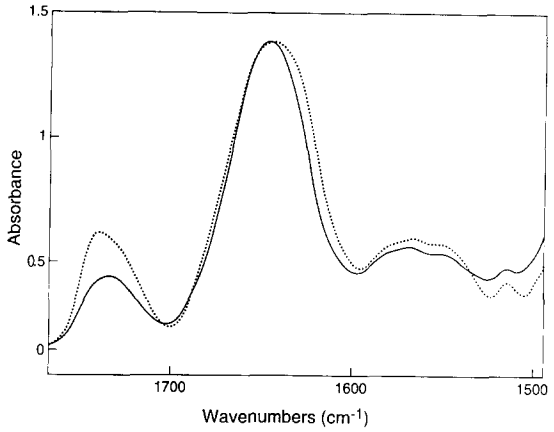

Fig. 5. Corrected amide-I spectra of nAChR-PC and nAChR-PCPA. Slight downfield broadening of the amide-I band occurs in the presence of phosphatidic acid.

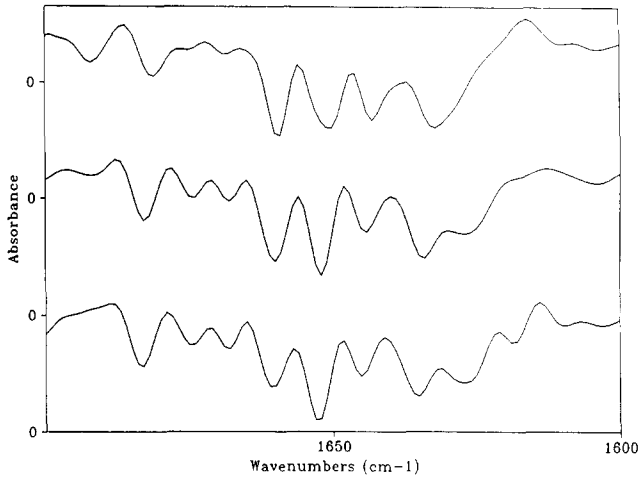

Fig. 6. Second derivative spectra of nAChR-PC (top), nAChR-PCPA (middle), and nAChR-PCPACH (bottom). The β-structure band at 1631 cm^{-1} in nAChR-PC split into a doublet in the presence of PA and PACH at positions 1633 cm^{-1} and 1626 cm^{-1}.

TABLE IV

Secondary structure estimates for nAChR-PC, nAChR-PCPA and nAChR-PCPACH in D_2O

The values were computed from the deconvolved and restored samples and represented as the mean ± S.D. Statistical analysis with the Mann-Whitney *U*-test showed that the α-helix content of nAChR-PCPACH was significantly higher than the samples not containing cholesterol, nAChR-PC and nAChR-PCPA ($P = 0.019$ and $P = 0.057$, respectively). Addtionally, we found that the β-structure content of samples containing PA, nAChR-PCPA and nAChR-PCPACH, was significantly higher than sample without PA, nAChR-PC ($P = 0.0095$).

Structure	nAChR-PC	nAChR-PCPA	nAChR-PCPACH
α-Helix	14.2 ± 1.6%	13.5 ± 1.8%	17.2 ± 1.3%
β-Structure	37.0 ± 1.5%	42.3 ± 1.3%	41.9 ± 2.1%
Turns and bends	28.5 ± 1.9%	25.6 ± 1.9%	25.3 ± 2.7%
Unordered	20.2 ± 2.7%	18.5 ± 2.6%	15.5 ± 2.4%

containing phosphatidic acid, nAChR-PCPA and nAChR-PCPACH, were significantly higher than the estimate for nAChR-PC (two-tailed $P = 0.0095$). The effect of cholesterol on β-structure was insignificant ($P = 0.89$).

There was also a slight increase in the α-helix content of nAChR when reconstituted into membranes containing cholesterol. The second derivative spectrum of nAChR-PCPACH showed a small increase in the α-helix band relative to neighboring peaks as compared to the nAChR-PC and nAChR-PCPA spectra (Fig. 5). Upon curve-fitting, the α-helix content in the sample containing cholesterol raised to 17% as compared to 14% for samples without cholesterol (Table IV). An equivalent decrease in unordered structure was also detected. Therefore, cholesterol may a cause a portion of the receptor to undergo an unordered-to-helical transition. Mann-Whitney *U*-analysis determined that the differences in α-helix content between nAChR-PCPACH were significantly different than the α-helix content of nAChR-PC and n-AChR-PCPA (two-tailed $P = 0.019$ and $P = 0.057$, respectively). Phosphatidic acid did not have a significant effect on the α-helix content ($P = 0.48$).

Secondary structure is invariable upon agonist binding

nAChR-PCPACH samples are known to exhibit ion-flux response and desensitization properties in reconstituted membranes [11,13]. Carbamylcholine chloride was added to the nAChR pellet at a final concentration of approx. 50 mM and the sample was analyzed by FTIR. Under these conditions, carbamylcholine will bind to the receptors and shift them rapidly into a desensitized state [11]. The corrected FTIR spectra of nAChR-PCPACH with and without the presence of carbamylcholine were similar while only minor relative differences in peak intensity were observed in their second derivative spectra (data not shown). The deconvolved and restored spectra of nAChR-PCPACH in the presence of carbamylcholine were curve-fit to yield secondary structure values. The average secondary structure values from the deconvolved and restored spectra were $18.8 \pm 1.4\%$ α-helix, $39.9 \pm 0.9\%$ β-sheet, $26.3 \pm 1.6\%$ turns and $15.2 \pm 0.6\%$ unordered. This is a 1.5% increase in α-helix and a 2.0% decrease in β-sheet for the ligand-bound receptor as compared to the receptor in the resting state. However, it was determined that these differences were not statistically significant with the Mann-Whitney *U*-test (two-tailed $P = 0.11$). The data from the present study are not strong enough to support the conclusion that carbamylcholine has an effect on secondary structure and further experiments are needed to determine if the small changes observed are meaningful. Complicating this analysis are the high concentrations of ligand necessary to ensure desensitization of the receptor, since carbamylcholine absorbs strongly at 1 704 cm^{-1}. Both D_2O and carbamylcholine must then be co-subtracted from the nAChR-PCPACH spectrum.

Discussion

In a previous study using the FTIR amide-III band, this laboratory estimated the secondary structure content of nAChR [34]. It was also determined that the secondary structure of the receptor could be altered by the lipid environment. Negatively-charged lipids and cholesterol, which are necessary for nAChR function, increased the β-sheet and α-helix content, respectively. This was the first direct observation that the properties of the lipid bilayer could affect the structure of a membrane protein.

In this study, we used the FTIR amide-I band to probe nAChR secondary structure. The amide-I band is significantly better for FTIR analysis than the amide-III band. The amide-I band has the advantage of a high signal, the absence of absorbances by lipids, and a strong consensus of agreement for the assignments of secondary structure elements.

In Table II, we compared our secondary structure estimates with estimates determined by other biophysical techniques. The α-helix values are fairly consistent for the experimental studies, but the computerized algorithms predict significantly more α-helix. The β-structure estimates vary widely among the techniques. Our results, as well as the CD studies, predict twice as much β-structure as the FTIR amide-III estimate.

FTIR spectrometry of proteins is commonly performed in D_2O solvent because H_2O absorbs strongly in the amide-I region, thus making accurate buffer subtraction difficult. Although subtraction is simpler in the weakly absorbing D_2O buffer, complications can arise due to incomplete deuterium exchange of the amide protons. Integral membrane proteins are especially susceptible to this problem because membrane spanning domains in the non-polar lipid bilayer may not be accessible to the bulk solvent. Due to the nature of this technique, unexchanged structures will skew the absolute secondary structure data. Therefore, we consider the values obtained in H_2O to be more accurate than the values obtained in the D_2O buffer. However, all other experiments were carried out in D_2O, because we were interested in examining the secondary structure differences between samples. Performing all experiments in H_2O would have provided absolute secondary structure values, but may have been subject to substantial error.

The differences observed between the secondary structure values determined in H_2O and D_2O were probably due to the incomplete exchange of all amide protons. The band corresponding to α-helix in D_2O contained only 14% of the amide-I envelope, whereas

in H_2O the α-helix band contained 19%. It is probable that the remaining 5% of the α-helix is a portion of unexchangeable transmembrane crossings and is left in the 1656 cm^{-1} band that is occluded by a strong 1659 cm^{-1} band ascribed to turns and bends. By subtracting an estimated 5% α-helix component from the 1659 cm^{-1} band in D_2O, the turns and bends value drops down to 24% which is similar to the value for the H_2O sample.

The factor of incomplete exchange is probably also responsible for the decrease in β-structure and increase in unordered structure in the D_2O sample as compared to the H_2O sample. The 1638 cm^{-1} band that represents unexchanged β-structure structure may be buried under the 1642 cm^{-1} unordered band in the D_2O spectrum. If we subtract 5% from the 1642 cm^{-1} band and add it to β-structure value to allow the β-structure values of the two samples to equal to 42%, the value for unordered structures in both samples will be 15%.

If we assume that the cytoplasmic and extracellular domains would be completely exchanged after 24 h, then we could maintain that the only unexchanged regions are the transmembrane domains that are shielded from the solvent by the lipid bilayer. In the four membrane-crossing model, it can be estimated that 20% of the receptor lies in transmembrane regions. However, the 5% unexchanged α-helix and 5% unexchanged β-structure observed in this study would only contribute half this amount. Some of this discrepancy may be explained by solvent accessibility of the amide protons of the transmembrane segments lining the ion channel or lying near the interfacial region of the lipid bilayer.

As outlined in the Introduction, the most probable structural model postulates that nAChR contains four transmembrane α-helices [26]. One of the alternate models proposes that there are two additional membrane crossings before the M1 region, one of which is entirely β-structure [35,36]. Our finding that a portion of the membrane domains may include β-structure is compatible with this model. However, it may also be in agreement with a four-crossing model that includes β-structure in its membrane domains. The simple Chou-Fasman method of secondary structure prediction suggests that nearly 85% of these putative membrane crossings would be in a β-structure conformation, while the Garnier-Osguthorpe-Robson method estimates that over 60% of the residues assume this conformation. Both methods strongly predict the M1 region to be almost completely β-structure. Only high resolution analytical techniques will be able to provide a description of the structure which lies in the transmembrane crossings.

We found that the presence of phosphatidic acid in reconstituted membranes could alter the β-structure

α	T	[H]	T	M	P	Q	W	V	[R	K]	I	F	I	D	T	I	P
β	T	[H]	T	M	P	N	W	I	[R	Q]	I	F	I	W	T	L	P
γ	T	[H]	S	L	S	E	[K]	I	[K	H]	L	F	L	G	F	L	P
δ	T	[H]	V	L	S	T	[R]	V	[K	Q]	I	F	L	E	[K]	L	P

Fig. 7. A moderately conserved cytoplasmic region of nAChR that may interact with the lipid bilayer. Positively-charged side chains may form ionic bonds with the negatively-charged phospholipids and force the neighbouring residues into a β-structure conformation. This type of local alteration may explain how specific lipids are necessary for maintaining nAChR function. In the figure, boxed residues are positively-charged.

content of the receptor. These results agree with those of Fong and McNamee who recorded a 4% increase under similar conditions, but using the amide-III band [34]. We feel that these findings indicate that ionic interactions between the positively-charged side chains of the protein and the negatively charged head group of the lipids could shift a portion of the receptor into a β-structure conformation. This local alteration may be necessary for allowing the receptor to achieve a functional conformation. It has previously been proposed that positively-charged side chains near the cytoplasmic side of the transmembrane region may interact with the head groups of negatively-charged lipids to anchor the domain into the bilayer [37]. Fong and McNamee postulated that residues 53–69 on the α-subunit which have a high β-structure amphiphilicity and positive-charge density could be the region interacting with the bilayer. However, this sequence is not conserved among the other subunits and could not account for the large change which corresponds to about 20 residues per subunit. We searched the nAChR sequences for a moderately conserved region containing a high density of positive charges and predicted to be β-structure by the computer algorithms. The best candidate was a 16-residue sequence beginning on the cytoplasmic border of M3 (Fig. 7). This region is believed to be near the lipid bilayer since it lies only six residues away from the putative M3 transmembrane domain. This cytoplasmic loop between M3 and M4 contains an amphipathic helix and multiple phosphorylation sites [38,39].

We also observed a change in the α-helix content of nAChR in the presence of sterols. Fong and McNamee found that the α-helix content increased from 17% to 20% when the receptor was reconstituted into membranes containing cholesterol. They postulated that the rigid sterol ring oriented parallel to the receptor axis may slide in between the helices at the lipid/protein interface and stabilize helix formation. These structural shifts may be necessary for the integrity of the ion channel and, thus, explain why cholesterol is essential for receptor function [34]. The present experiments support this hypothesis, since we detected a decrease in unordered structure with corresponding increases in

helical structure. The 3% observed increase coincides with about 15 residues per subunit. This is approximately two-thirds the number of residues found in a predicted transmembrane crossing.

We did not find any significant secondary structure changes when nAChR-PCPACH was incubated with a carbamylcholine concentration know to desensitize the receptor. These results are in agreement with the data from other biophysical techniques that have been employed to study the conformational changes associated with desensitization. Cryoelectron microscopy has shown that nAChR undergoes only slight quaternary rearrangement in the presence of carbamylcholine [14]. The agonist induced the synaptic portion of the δ-subunit to undergo a 10° tangential tilt relative to the receptor axis without any observable changes in the secondary and tertiary structure. Additionally, circular dichroism data has shown that significant changes in secondary structure are not occurring during ligand binding [16]. However, circular dichroism, as well as FTIR spectroscopy, are limited to finding only net changes in secondary structure as they are not able to detect compensatory conformational changes.

FTIR spectrometry is a useful tool for examining the structure of proteins, especially those that have not yet undergone high resolution analysis. In this paper, FTIR spectrometry has allowed us to deduce nAChR secondary structure and examine conformational changes induced by specific lipids. Utilizing biochemical, biophysical and molecular genetic techniques we hope to determine the nature of these interactions and to localize the domains of nAChR that interact with the membrane.

Acknowledgements

The authors thank Dr. John Crowe (Department of Zoology, University of California, Davis) for the use of his FTIR spectrometer and Dr. Enrique Ochoa and Dr. Anil Bhushan for their helpful discussions. We thank Alan Chui and Jordan Scalo for performing nAChR purifications. This research was supported by a research grant to M.G.M. from the National Institutes of Health (NIH Grant 13059) and a Jastro-Shields graduate research scholarship and NIH Training Grant (NIH 1-T32GM08343) to D.H.B.

References

1 Strange, P.G. (1988) Biochem. J. 249, 309–318.
2 Brisson, A. and Unwin, P.N.T. (1984) J. Cell Biol. 99, 1202–1211.
3 Karlin, A., Holtzman, E., Yodh, N., Lobel, P., Wall, J. and Hainfeld, J. (1983) J. Biol. Chem. 258, 6678–6681.
4 Claudio, T., Ballivet, M., Patrick, J. and Heinemann, S. (1983) Proc. Natl. Acad. Sci. USA 80, 1111–1115.
5 Giraudat, J., Dennis, M., Heidmann, T., Chang, J. and Changeux, J. (1986) Proc. Natl. Acad. Sci. USA 83, 2719.
6 Leonard, R.J., Labarca, C.G., Charnet, P., Davidson, N. and Lester, H.A. (1988) Science 242, 1578.
7 Giraudat, J., Montecucco, C., Bisson, R. and Changeux, J. (1985) Biochemistry 24, 3121.
8 Li, L., Schuchard, M., Palma, A., Pradier, L. and McNamee, M.G. (1990) Biochemistry 29, 5428–5436.
9 Dalziel, A.W., Rollins, E.S. and McNamee, M.G. (1980) FEBS Lett. 122, 193–196.
10 Criado, M., Eibl, E. and Barrantes, F.J. (1982) Biochemistry 21, 3622–3629.
11 Ochoa, E.L.M., Dalziel, A.W. and McNamee, M.G. (1983) Biochem. Biophys. Acta 727, 151–162.
12 Ellena, J.F., Blazing, M.A. and McNamee, M.G. (1983) Biochemistry 22, 5523–5535.
13 Ochoa, E.L., Chattopadhyay, A. and McNamee, M.G. (1989) Cell. Mol. Neurobiol. 9, 141–78.
14 Unwin, N., Toyoshima, C. and Kubalek, E. (1988) J. Cell Biol. 107, 1123–1138.
15 McCarthy, M.P. and Stroud, R.M. (1989) J. Biol. Chem. 264, 10911–10916.
16 Mielke, D.L. and Wallace, B.A. (1988) J. Biol. Chem. 263, 3177–3182.
17 Mitra, A.K., McCarthy, M.P. and Stroud, R.M. (1989) J. Cell Biol. 109, 755–774.
18 Toyoshima, C. and Unwin, N. (1990) J. Cell Biol. 111, 2623–2635.
19 Byler, D.M. and Susi, H. (1986) Biopolymers 25, 469–487.
20 McNamee, M.G., Jones, O.T. and Fong, T.M. (1986) in Ion Channel Reconstitution (Miller, C. ed.), pp. 231–273, Plenum, New York.
21 Lowry, O.H., Rosebrough, N.J., Farr, A.L. and Randall, R.J. (1951) J. Biol. Chem. 193, 265–275.
22 McClare, C.W.F. (1971) Anal. Biochem. 39, 527–530.
23 Dong, A., Huang, P. and Caughey, S. (1990) Biochemistry 29, 3303–3308.
24 Holloway, P.W. and Buchheit, C. (1990) Biochemistry 29, 9631–9637.
25 Savitsky, A. and Golay, M. (1964) Anal. Chem. 36, 1627.
26 Noda, M., Takahashi, H., Tanabe, T., Toyosato, M., Kikyotani, S., Furutani, Y., Hirose, T., Takashima, H., Inayama, S., Miyata, T. and Numa, S. (1983) Nature 302, 528–532.
27 Devereux, J., Haeberli, P. and Smithies, O. (1984) Nucleic Acids Res. 12, 387–395.
28 Chou, P.Y. and Fasman, G.D. (1978) Adv. Enzymol. 47, 45–148.
29 Nishikawa, K. (1983) Biochim. Biophys. Acta 748, 285–299.
30 Garnier, J., Osguthorpe, D.J. and Robson, B. (1978) J. Mol. Biol. 120, 97–120.
31 Krimm, S. and Bandekar, J. (1986) Adv. Protein Chem. 38, 181–364.
32 Wantyghem, J., Baron, M.-H., Picquart, M. and Lavialle, F. (1990) Biochemistry 29, 6600–6609.
33 Holloway, P.W. and Mantsch, H.H. (1989) Biochemistry 28, 931–935.
34 Fong, T.M. and McNamee, M.G. (1987) Biochemistry 26, 3871–3880.
35 Criado, M., Hochschender, S., Sarin, V., Fox, J.L. and Lindstrom, J. (1985) Proc. Natl. Acad. Sci. USA 82, 2004–2008.
36 Pedersen, S.E., Bridgman, P.C., Sharp, S.D. and Cohen, J.B. (1990) J. Biol. Chem. 265, 569–581.
37 Ballesteros, J. and Weinstein, H. (1992) Biophys. J. 62, 127–129.
38 Finer-Moore, J. and Stroud, R.M. (1984) Proc. Natl. Acad. Sci. USA 81, 155.
39 Huganir, R.L. and Miles, K. (1989) Crit. Rev. Biochem. Mol. Biol. 24, 183–215.
40 Yager, P., Chang, E.L., Williams, R.W. and Dalziel, A.W. (1984) Biophys. J. 45, 26–28.
41 Bhushan, A. and McNamee, M. (1993) Biophys. J. 64, 716–723.